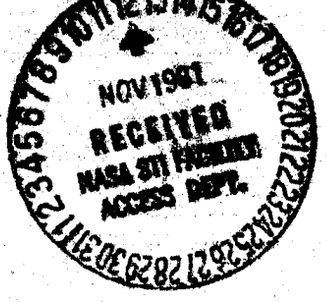

DEPARTMENT OF CIVIL ENGINEERING
HOWARD UNIVERSITY
WASHINGTON D C

Howard University

STUDY OF FOLDABLE ELASTIC TUBES FOR LARGE SPACE STRUCTURE APPLICATIONS

FINAL REPORT

For

PHASE III

by

Irving W. Jones
Steve O. Mitchell

September 1981

Conducted Under NASA Grant NSG 1320

Principal Investigator:

Irving W. Jones
Professor, Civil Engineering
Howard University

NASA Technical Officer:

Joseph E. Walz
Structures and Dynamics Division
Langley Research Center

ABSTRACT

This report presents the results of the final phase of a three-part investigation of foldable structural members. The project has focused attention on one particular type which appears to be suitable for use in self-deploying space structures. It has been referred to in previous literature as a bi-convex foldable elastic tube (BFET). The tube is cylindrical with a cross-section that is lenticular-like with flared edges. It is capable of being flattened in the center and folded compactly, storing up strain energy in the process. Upon removal of constraint, it springs back to its original straight configuration, releasing the stored strain energy.

Phase III of the investigation, which is the work reported herein, concentrated on the BFET structural stability. Specifically, it consisted of a series of buckling tests to determine initial buckling loads, collapse loads and the buckling mode, and it relates these to the material and geometric parameters of the tube. The tests showed that this type of tube has good resistance to buckling, with the initial buckling loads all falling within or above the range of those for comparable circular cylindrical tubes.

TABLE OF CONTENTS

LIST OF ILLUSTRATIONS

FIGURES (Continued) Page

LIST OF TABLES

1. INTRODUCTION

1.1 Background

The foldable structural members being evaluated in this investigation are among candidate types for use in a so-called strain-energy-deployable truss structure; that is, a type of truss structure that can be folded up into a dense package with some members being folded sharply in half, remaining elastic and thus storing strain energy. The folded structure is restrained in this configuration for launch into space, whereupon it is released to deploy through the utilization of the stored strain energy.

The particular type of foldable member investigated here is one which has been called in previous literature a bi-convex foldable elastic tube (BFET), a closed thin-walled cylindrical tube made up of circular cylindrical segments which together form the lenticular-like shape shown in Fig. 1.1. Earlier research on the BFET has been reported in refs. 1 through 7. The concept of employing as a foldable member a tube whose cross-section can be flattened and thus remain elastic is attractive because of its simplicity. It dispenses with the need for a mechanical hinge or spring. However, despite early optimistic results with this type of tube (refs. 1, 2), the most recent study cited above, ref. 3, and the present study revealed a serious shortcoming. That is, when the tube had almost completed its unfolding action and was within about 15 degrees of becoming straight, and the previously flattened center region was snapping back and to its original shape, the tube had a tendency to settle into a state of stable equilibrium in a slightly buckled configuration. Ref. 3, which documents an extensive experimental and theoretical investigation of the BFET, reported repeated occurences of this phenomenon.

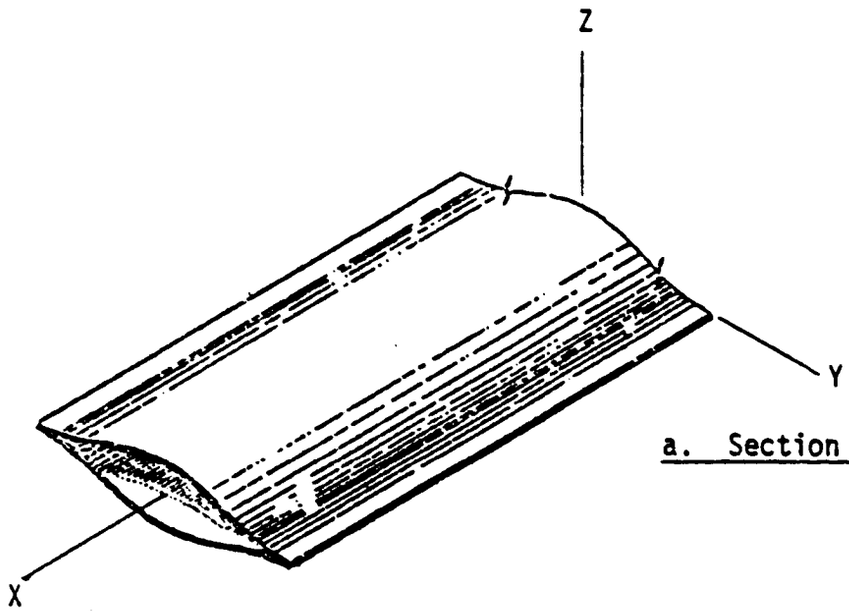

a. Section of BFET

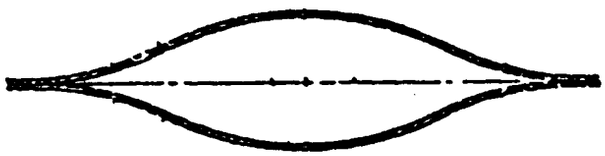

b. Tube Cross-section

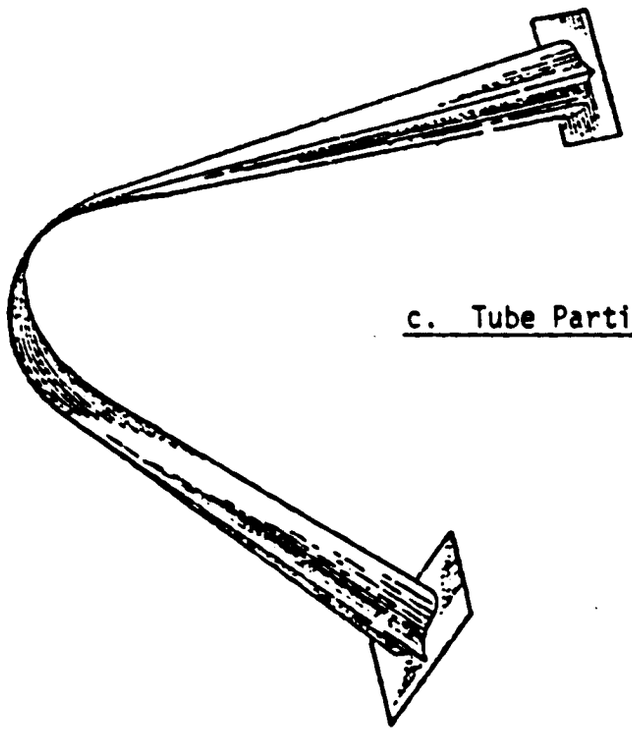

c. Tube Partially Folded

Fig. 1.1 Bi-Convex Folcable Elastic Tube (BFET)

In the initial work of the present project, which has been called Phase ., (refs. 4, 5), further occurences of this behavior were noted, thus clearly indicating the need for a design modification or abandonment of the design.

Phase II of this project, (refs. 6, 7), consisted of making various modifications to the BFET in an effort to eliminate the buckling problem. It was found that by cutting narrow slots in the central region of the tube, in the longitudinal (x, in Fig. 1.1a) direction, the buckled state could be avoided and the tube would deploy successfully. These slots serve to relieve the high compressive strains that develop in the tube in the lateral (y) direction as its center region attempts to snap through. After discovering that this approach was successful, the subsequent work was directed to determining the optimum width, length and location for the slots and the loss in strengtr and stiffness due to their insertion, to re-test the tube specimens under the same conditions as was initially done, and to analyze the results in order to relate the strain energy released to the tube geometry. The results of these efforts are detailed in sections 2 through 5 of a previous report to NASA, ref. 6.

The conclusion of the project, the investigation of the structural stability of the tube, i.e., its resistance to local or shell buckling, has been called Phase III and is documented in this report. Some material from the reports on previous parts of the project have been included for completeness.

2. TEST SPECIMENS

2.1 Geometry

The cross-section shape of the BFET can be uniquely defined by any two of the parameters R, λ and f, shown in Fig. 2.1a. For this analysis, the independent parameters were chosen as R, the arc radius, and f, a measure of the tube flatness, which is defined as $f = \lambda/R$, where λ is the offset of the circular arc center from the mid-plane. The value of f can vary from 0 to 1, with the extremes being f = 0 (a cross-section whose central portion is round) and f = 1 (a completely flat cross-section), as illustrated in Fig. 2.1b.

For this investigation, it was desired to have an array of 30 to 40 shapes varying in both size and in flatness, but having the same wall thickness, t = 0.010 inches, and length, ℓ = 48 inches.

The wall-thickness, length and range of cross-section sizes were all established such that the test specimens would represent the center region of a full scale large space truss member, as it is expected to be proportioned, according to preliminary NASA studies (e.g., ref. 8). The folding action in, say, a 15' to 20' member would be expected to take place well within the 48" length that was assigned to these specimens (Fig. 2.1c).

Due to (1) inaccuracies in forming of the specimen halves by the rubber pad process, (2) small changes in shape that occured when the specimens were handled for seam welding, and (3) further small changes in the heat treating process, the specimens, when ready for testing, did not have exactly the cross-section contours that were originally designed. But, as can be seen from Table 2.1, the set of 33 specimens, covered a wide enough range of radii ($1.41" < R < 5.91"$) and flatnesses ($0.07 < f \leq 0.89$), to satisfy the original objectives in those areas. As is shown, the specimens were separated into

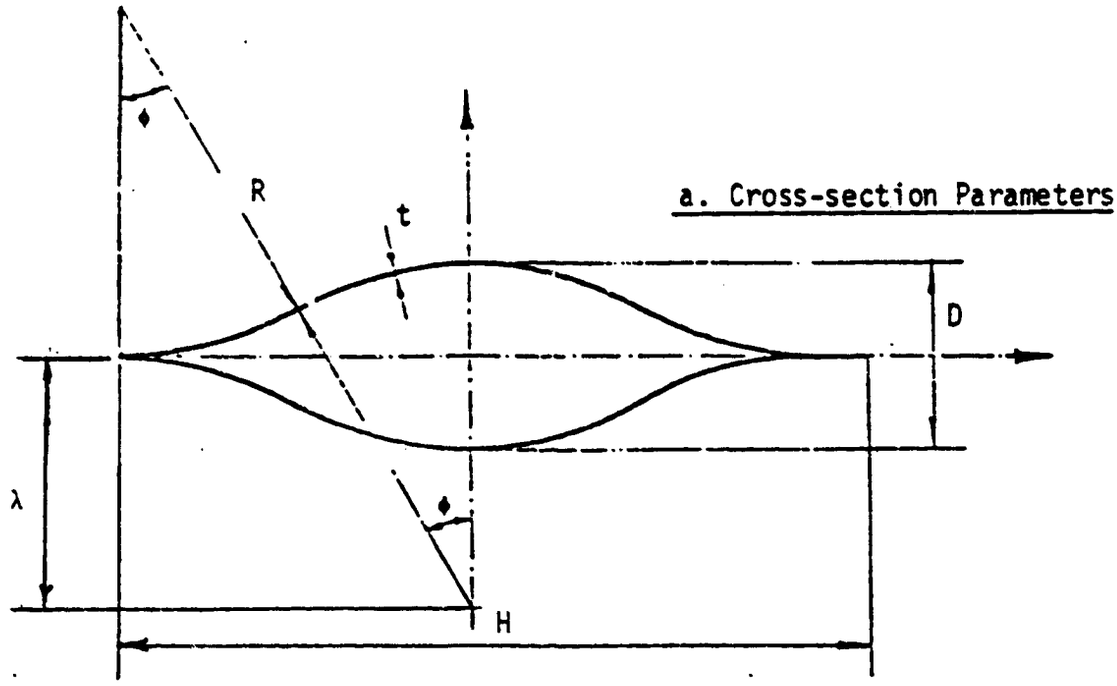

a. Cross-section Parameters

R = arc radius of curvature
λ = mid-plane to curvature center
f = λ/R = flatness
ϕ = arc opening angle

H = overall width
D = overall depth
S = arc length of ½ section
t = wall thickness

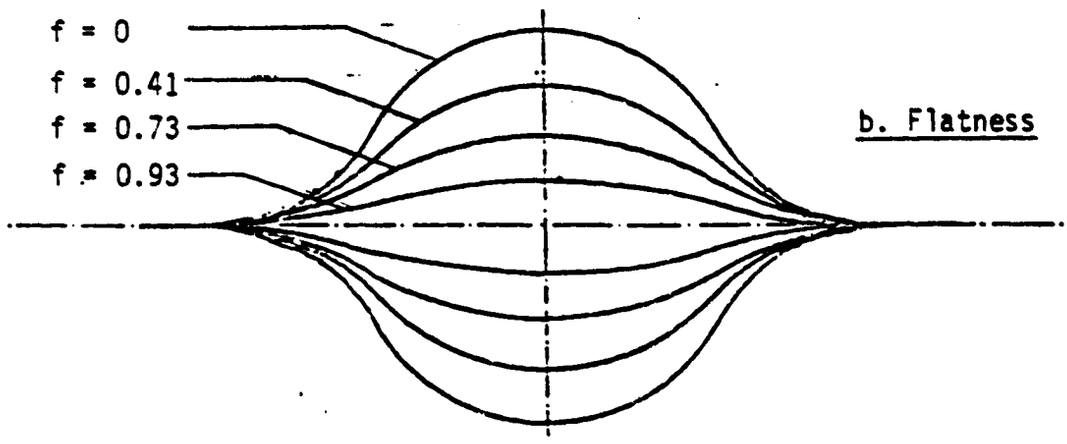

b. Flatness

c. Length

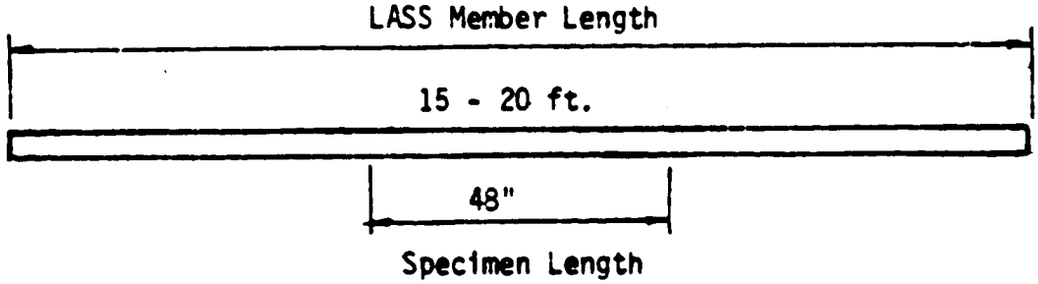

Fig. 2.1 TEST SPECIMEN GEOMETRY

TABLE 2.1
TABLE SPECIMEN DATA

Specimen No.	Radius, R in.	Offset, λ in.	Flatness, f	Slot Configuration (See Fig. 2-2)
VERY FLAT				
NA-1	5.91	5.27	0.89	SS
NA-2	5.71	5.04	0.88	SS
NB-1	3.58	2.85	0.80	SS
NB-2	3.45	2.65	0.77	
NB-3	3.76	2.57	0.68	SS
NB-4	3.53	2.38	0.67	
NB-5	3.56	2.23	0.63	
MODERATELY FLAT				
NC-1	1.80	1.08	0.60	SS
NC-2	1.82	1.05	0.58	FE
NC-3	1.88	1.02	0.54	DS
ND-1	1.65	0.82	0.50	
ND-2	1.80	0.89	0.49	SS
ND-3	1.76	0.85	0.48	FE
NE-1	2.76	1.42	0.51	
NE-2	2.71	1.16	0.43	SS
NE-3	2.49	1.55	0.62	FE
NF-1	1.50	0.79	0.52	SS
NF-2	1.58	0.69	0.44	FE
NF-3	1.56	0.67	0.43	SS
NF-4	1.57	0.66	0.42	
NF-5	1.41	0.53	0.38	SS
NF-6	1.54	0.57	0.37	SS
SLIGHTLY FLAT				
NG-1	2.03	0.65	0.32	FE
NG-2	2.00	0.57	0.28	
NG-3	2.40	0.82	0.34	SS
NG-4	2.14	0.59	0.27	SS
NG-5	2.42	0.40	0.16	SS
NG-6	2.50	0.49	0.20	FE
ROUND				
NH-1	2.00	0.35	0.17	DS
NH-2	2.21	0.36	0.16	
NH-3	2.10	0.20	0.09	FE
NH-4	1.86	0.18	0.10	SS
NH-5	1.66	0.12	0.07	

groups with similar radii (R) and offsets (λ). Thus, they could be given identifications according to group (NA through NH) indicating general size and degree of flatness, the cross-section properties having been measured directly from penciled outlines of the specimen ends.

2.2 Material and Fabrication

The success of the foldable elastic tube concept depends upon the tube remaining elastic throughout when it is folded sharply in half through 180°. Therefore, the tube must be made of a material with high yield strain (high yield stress and/or low modulus of elasticity). Also, fabrication and strength-to-weight considerations dictate that the material have adequate formability, weldability and low density. The material chosen for this study, a stainless steel, possesses all of these qualities, as to titanium, some hard copper alloys and composites. The selected material, 17-7PH stainless, proved to be satisfactorily formable in the annealed condition and hardenable to sufficiently high strength levels by the use of a standard heat treatment. Fabrication practices for 17-7PH are the same as for other chromium-nickel stainless steels. Specified mechanical properties at room temperature, as well as properties determined from tests on the material used in this project are shown in Table 2.2. To obtain the latter, standard tensile coupons were cut from sheets of the 17-7PH material that had been subjected to the heat-treatment along with the test specimens. These were tested and the results were as shown. The yield strengths averaged 179,500 and 189,500 psi in the longitudinal (roll) and transverse direction respectively. The yield strength in the roll direction was a little below the supplier's specified value of 185,000 psi, but was sufficiently high for this application (See ref. 9).

The specimen halves were formed by the Guerin, or rubber pad, process.

TABLE 2.2

ARMCO 17-7PH STAINLESS STEEL PROPERTIES

SPECIFIED MECHANICAL PROPERTIES, ROOM TEMPERATURE

Typical Properties

Condition	Ultimate Tensile Strength, psi (Mpa)	0.2% Tensile Yield Strength psi (Mpa)	Elongation % in 2" (50 mm)	Hardness, Rockwell
ANNEALED	130,000 (896)	40,000 (276)	35	B85
TH1050	200,000 (1379)	185,000 (1276)	9	C43
RH950	235,000 (1620)	220,000 (1517)	6	C48

PROPERTIES OF MATERIAL USED IN THIS INVESTIGATION

Condition	Ultimate Tensile Strength, psi (Mpa)	0.2% Tensile Yield Strength psi (Mpa)	Elongation % in 2" (50 mm)	Hardness, Rockwell
ANNEALED	Longitudinal:			
	146,000 (1006)	54,000 (372)	31	B75
	Transverse:			
	146,000 (1006)	53,000 (365)	28	B75
TH1050	Longitudinal:	179,500		
	Transverse:	189,500		

Rubber pad forming employes either a monclithic or layered rubber pad encased in a heavy retainer. The pad acts in the manner of the recessed part of a die. A form block acts as the punch in conventionel forming. The block is secured either to the ram or the platen of the press. The blank (the piece to be formed) is positioned between the form block and the rubber pad, and as the two are brought together, the blank is forced into the rubber pad and is bent into the shape of the form block. The rubber acts somewhat like a hydraulic fluid in exerting nearly equal pressure over the surface of the blank.

The forming set-up was as follows. A multi-layered rubber pad was encased in the steel retainer box. The box was supported on two steel horses which were available in the laboratory. Above the retainer, the contured form block was secured to the 4' x 4' head plate of the 600,000 lb. capacity universal testing machine, which was used as the press. Each rectangular sheet, or blank, was positioned on the form block by inserting its two locating holes into the corresponding two locating pins (one at each end) on the block. The blank was lubricated with drawing wax prior to fastening. As the press was lowered, the blank was formed into the shape of the block; upon removal of the pressure, it sprang back to a shape of lesser curvature. The form blocks were designed with shapes such that, theoretically, the specimen half should relax into the originally planned shape after springback.

2.3 Slot Configurations

The idea of cutting slots in the tubes as a stress alleviation device suggested itself during observations of the earlier tests on the closed tubes (ref. 4). Slotting the tubes makes the snap-through phase of deployment easier by reducing the compressive strains and stresses in the lateral direction.

The arrangements of the slots were established in such a way that the

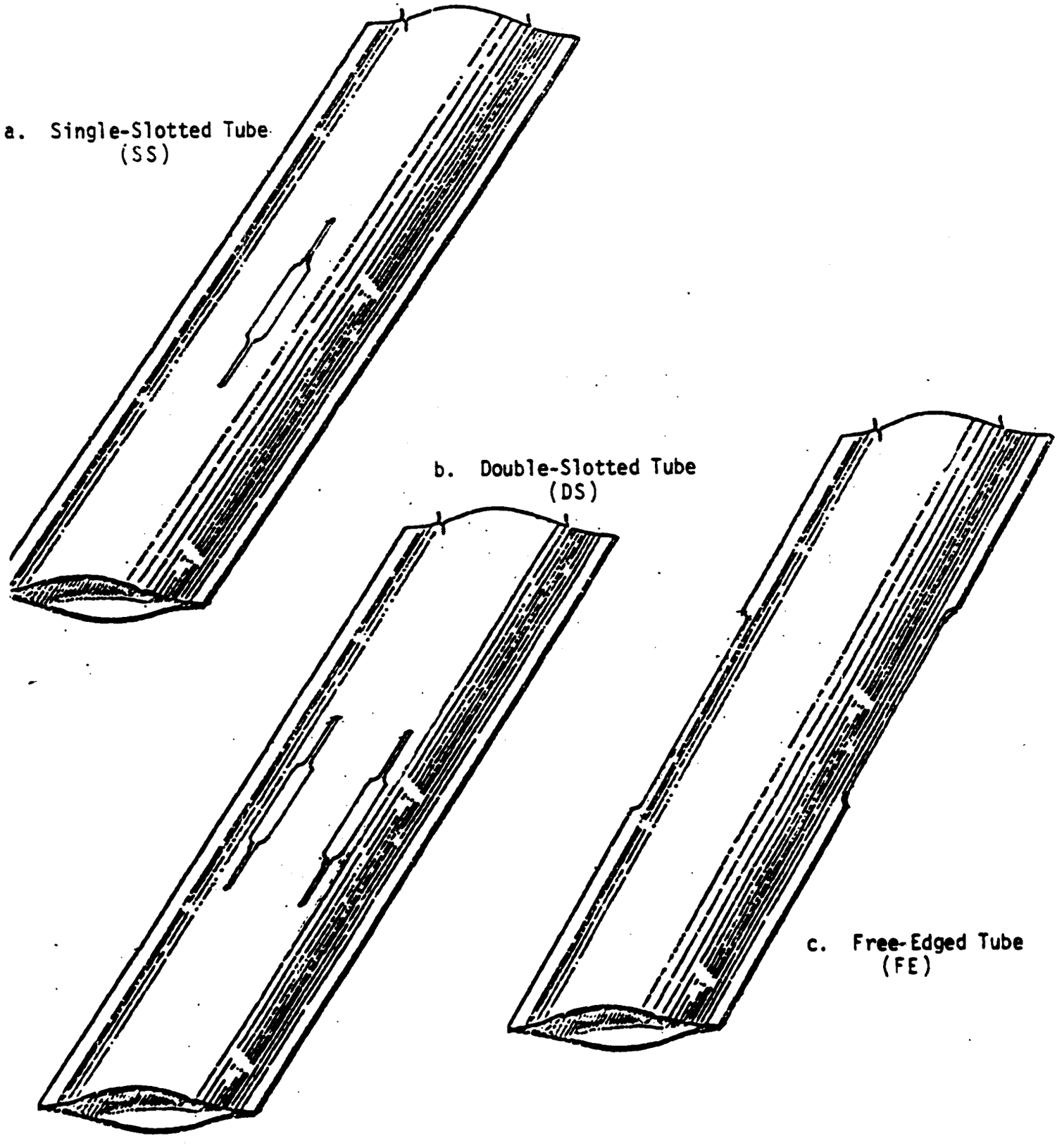

Fig. 2.2 MODIFIED BFET CONFIGURATIONS

tubes might both deploy fully and maintain sufficient bending and torsional stiffness. Three configurations, as shown in Fig. 2.2, were tried. For convenience, these are referred to in later sections of the report as follows:

- Free-Edged (FE) - The seam weld and material 1/16 inch inside it cut away to produce free edges on upper and lower halves of tube.
- Single-Slotted (SS) - One slot cut on each side (compression and tension (or +Z and -Z) sides of tube along its center-line, or X - X axis.
- Double Slotted (DS) - Two slots cut on each (+Z and -Z) sides of tube along the line of tangency of the circular cylindrical sections.

The workability of these three configurations, as well as the required width and length of the slots was investigated through an incremental process. Initially, the slots in the single and double-slotted tubes were made 1/16 inch wide, and for all three configurations the incisions were eight inches long. Although the slots are needed only on the side of the tube that is in compression when folded, they were cut on both sides to preserve symmetry and resistance to buckling.

In the incremental process, the central four inches of the slots were widened by a small amount at at a time to produce the slot shape shown in Fig. 2.3. The slot in each specimen was incrementally widened until a smooth

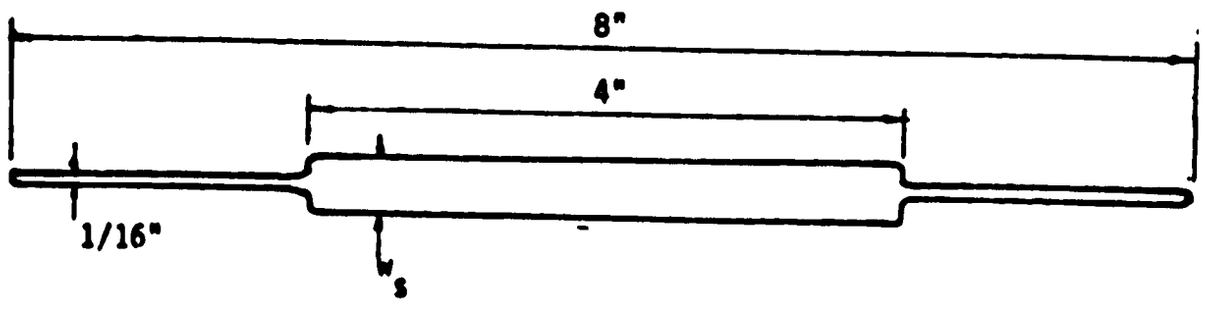

Fig. 2.3 Slot Configuration

deploying action was achieved. The final widths of the slots ranged between ¼ inch and 7/16 inch. The required width turned out to be inversely proportional to the specimen flatness, but bore no discernable relationship to any other parameters, at least within the range of specimen sizes tested. The approximate relation for slot width w_s was:

For $1.5 < R < 6$, and

$$f \sim 0.8: \quad w_s \sim 1/4"$$
$$f \sim 0.6: \quad w_s \sim 3/8"$$
$$f \sim 0.4: \quad w_s \sim 7/16"$$

3. TEST APPARATUS AND PREPARATION

3.1 Description of Set-up

An assembly drawing of the compression testing machine and associated hardware is shown in Fig. 3.1, and a photograph of it in Fig. 3.2. A diagram of the instrumentation is shown in Fig. 3.3. The compressive load was delivered by a Karol-Warner 25,000 lb. (111.15kN) capacity screw-type compression testing machine. A strainsert Fl. 25U-3DP 25,000 lb. (111.25kN) capacity calibrated load cell was mounted between the crosshead of the machine and a ground steel plate, to which it was bolted. At the lower end of the assembly, a rectangular ground steel plate was mounted to the circular base plate of the machine. A leveling assembly, which rests on this plate, consists of three leveling screws equally spaced at 120° angles around a 13 inch (330 mm) diameter circle, connected to a leveling plate. This assembly provided for plane adjustment of the plate orientation. Between the upper and lower plates was mounted a calibrated Schaevitz linear variable displacement transformer (LVDT), attached as shown, to measure the end shortening of the test specimen. Signals from the load cell and the LVDT were carried to a Hewlett Packard 7004B X-Y Recorder, which plotted the load versus end shortening (P-e) curve.

During the running of a trial test, oscillations in the x-y plot was observed. These oscillations were of such magnitude that an accurate plot of load versus and shortening could not be obtained. The problem was due to the specimen buckling at a far lesser load than the capacity of the load cell, and lesser level of sensitivity at which the x-y recorder modules could respond. At 25,000 pounds (111.25kN), a signal of 22.5 mv was produced and sent to the recorder. But, since the specimens buckled at about 1/25 to 1/12 the

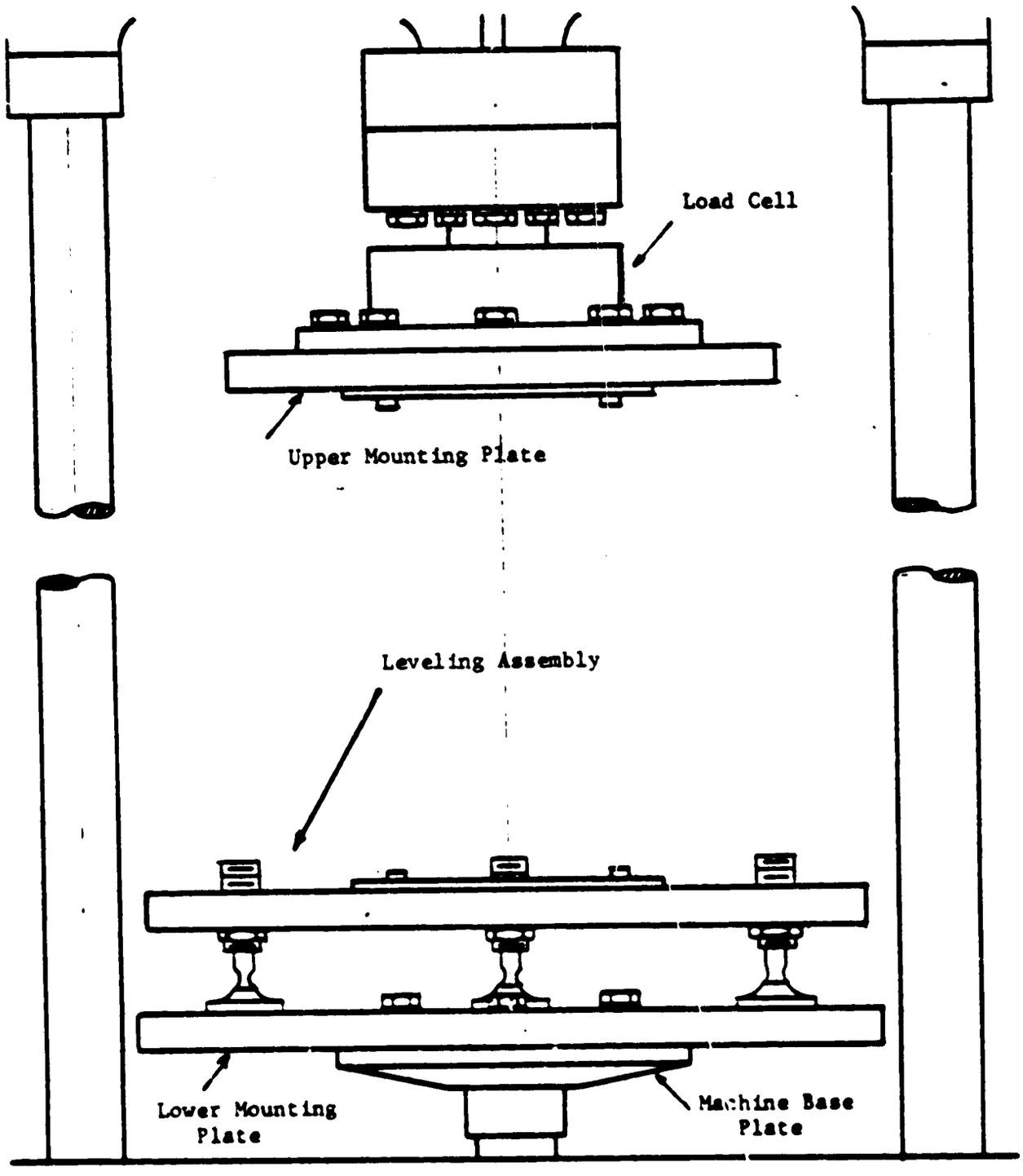

Fig.3.1 Compression Testing Machine and Accessories

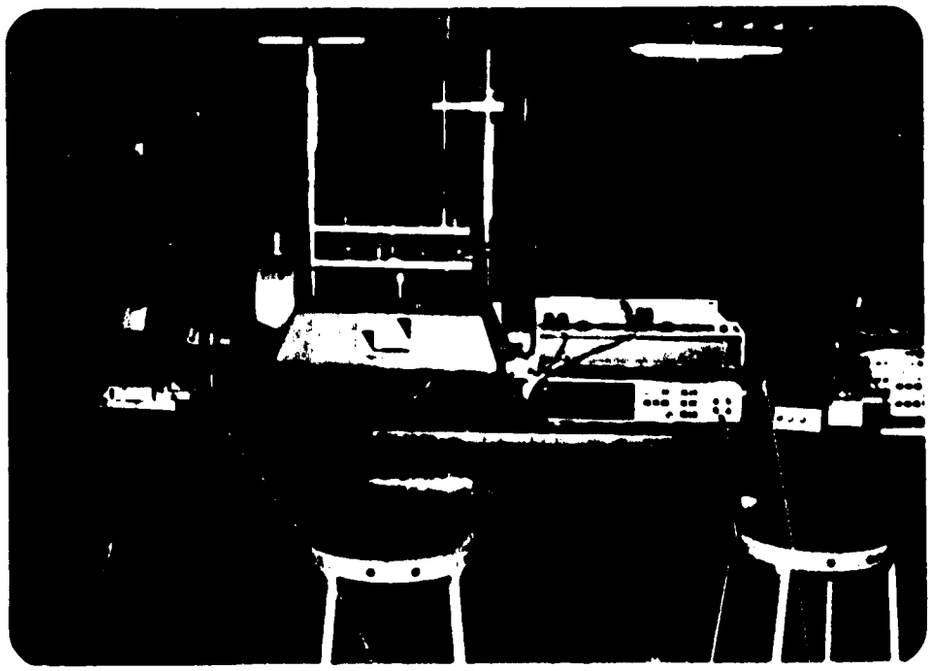

Fig. 3.2 Compression Machine and Instrumentation

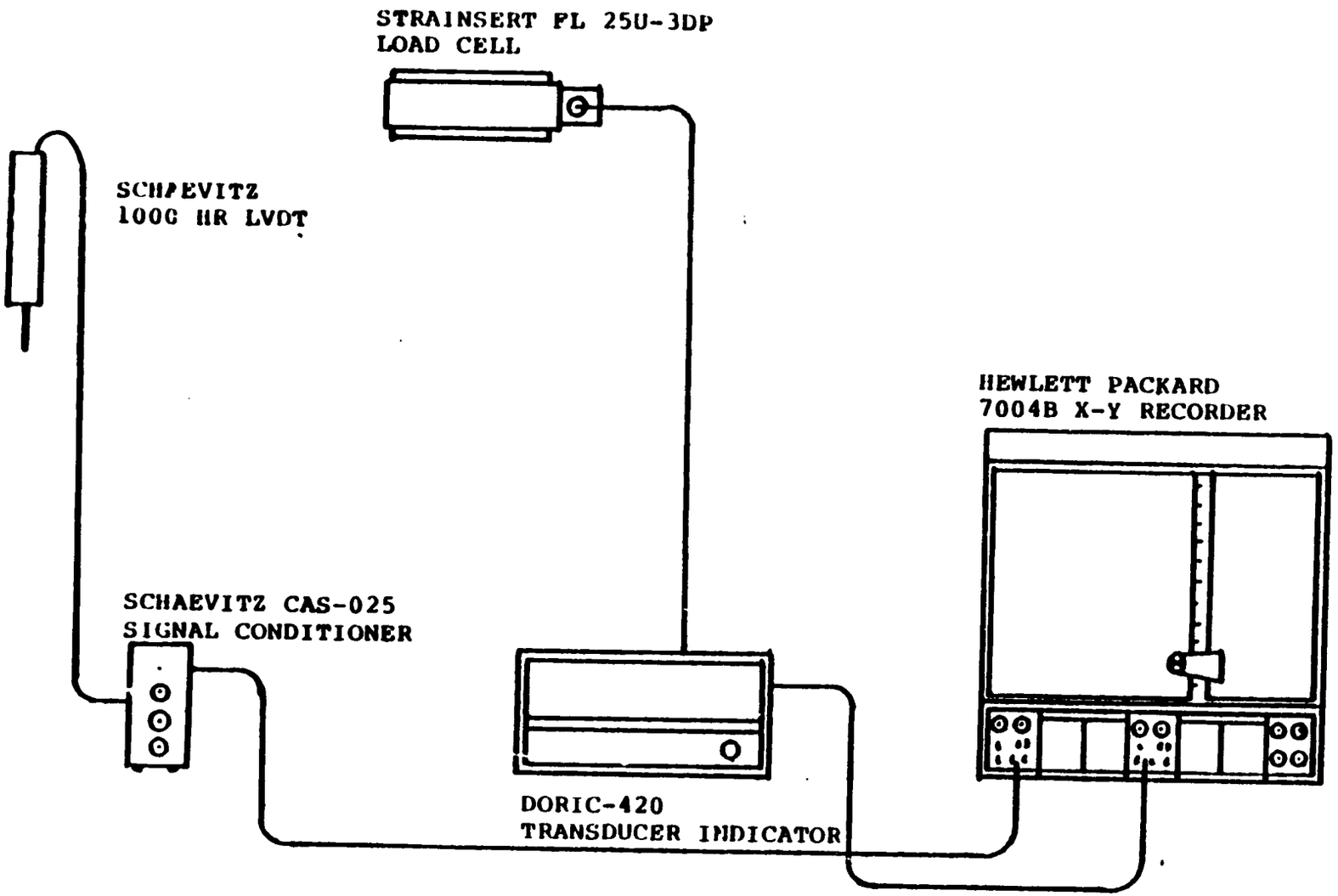

Fig.3.3 INSTRUMENTATION DIAGRAM- BUCKLING TESTS

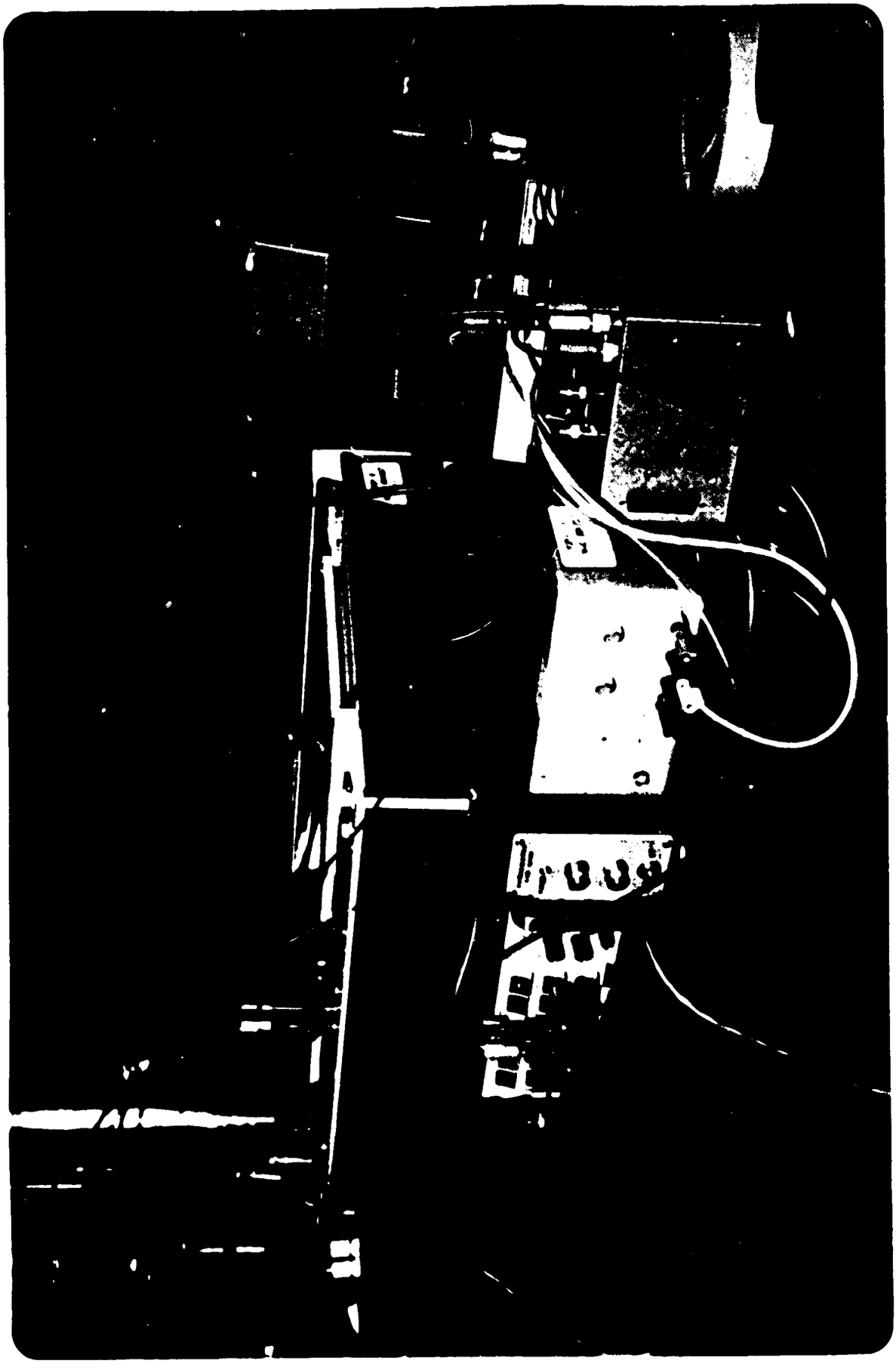

Fig. 3.4 Modified Instrumentation

capacity of the load cell, a signal in the range of only 1 mv was being sent to the recorder. Therefore, the recorder picked up noise instead of the weak signal, thus producing oscillations. Two solutions were considered. One was to obtain a smaller load cell (10,000 lb, 44.5 kN, cap.); the second was to boost the signal before it went to the recorder. It was decided to introduce additional modules to boost the signal. An instrumentation amplifier, assembled by one of our electronics technicians, was connected. Also connected was a Sprague 850WA4 Decade Inductor, a Hycor 103 Decade Inductor, and a Sprague 34D Capacitor to further reduce the noise. Fig. 3.4 shows a photograph of the modifications to the testing apparatus.

3.2 Specimen Preparation and Mounting

The specimen was mounted into an alignment jig, which was simply a flat ground metal base plate 6x9 inches (152 x 229mm) placed horizontally, with a plywood sheet 6x15 inches (152 x 381mm) mounted squarely at right angles to it and standing vertically. A drawing and a photograph of the potting apparatus are given in Fig. 3.5 and 3.6 respectively. The specimen was encased squarely onto two steel end plates using a low-melting-point epoxy. One end plate was first placed into the jig base plate, and a dam formed from pieces of rubber was placed down to contain the epoxy. The specimen was positioned into the jig with its edges firmly in the guide grooves, ensuring that they were perpendicular to the end plates. Epoxy was poured into the trough and the specimen was lowered into it with its edges still in the grooves. When the epoxy hardened, the specimen was removed, inverted and the process repeated with the other end plate.

The specimen was then ready to be mounted into the testing machine. The upper plate of the testing machine was already squarely aligned with the load cell. The specimen was placed in the testing machine, and the end plate holes were aligned with those on the base plate. Screws were put in to keep The specimen from moving while testing progressed.

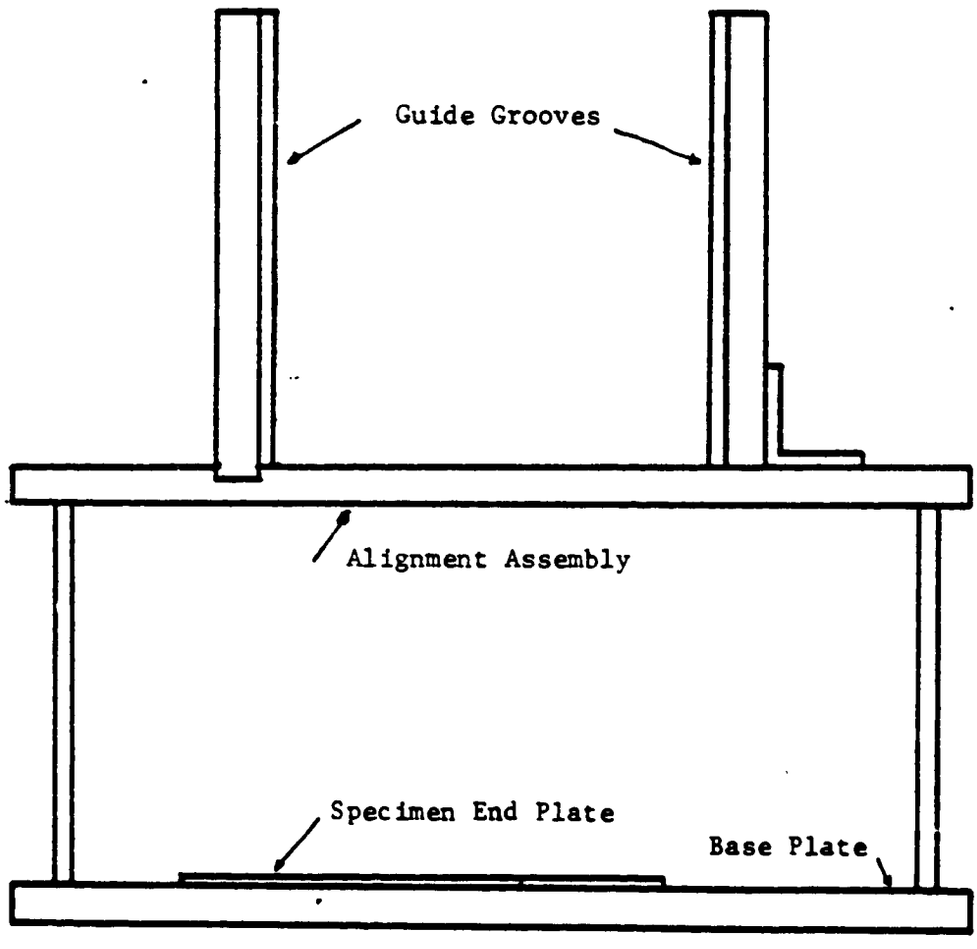

Fig.3.5 Alignment and Mounting Jig

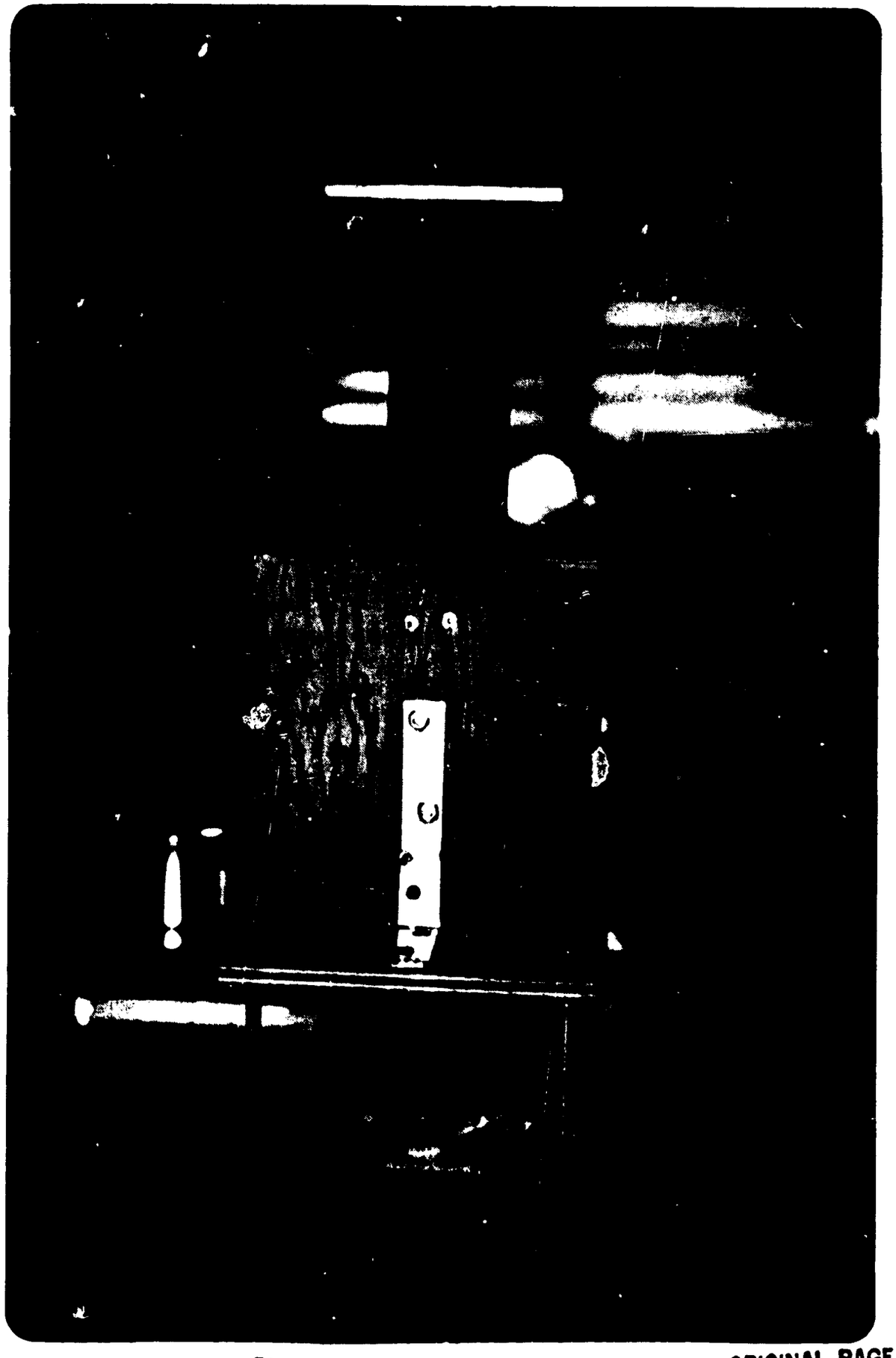

Fig. 3.6 Alignment and Mounting Jig

4. BUCKLING TEST PROCEDURE AND RESULTS

4.1 Buckling Test Procedure

The testing apparatus was turned on and allowed to warm up and stabilize before the testing started. The calibration of the units was then checked and the specimen mounted. The specimen was aligned in the compression machine and trial buckled to determine if the alignment was accurate, then unloaded. The specimen was preloaded to 50 lbs. (223N) to pick up the slack in the system. It was noticed that along with the advantages of the amplifier, a backlash was developed. The x-y recorder was set up to compensate for the preload also. Each of the specimens was tested twice at three different loading rates.

1. 0.014 inches/min. (0.355 mm/min.)
2. 0.023 inches/min. (0.584 mm/min.)
3. 0.030 inches/min. (0.762 mm/min.)

After each test, the alignment was adjusted if the specimen had not buckled symmetrically.

On the specimen NG-2, strain gages were placed around the slots to examine the stress distribution around the perimeter. The same procedure as before was used except that the loading was stopped after every 200 lb. (890 N) increment so that the strains could be read.

4.2 Determination of Required Specimen Length

It was necessary to determine a minimum acceptable length for the specimens in order to ensure that the buckling load would not be influenced by the specimen's end conditions. An initial specimen (NE-1) was cut to 24 inches (610mm), potted and tested. This length was the maximum length limit of the compression testing machine. Next the specimen was cut to

21 inches (533 mm), re-potted, re-tested, and the process repeated for 18 inches (457 mm). Fig. 4.1 shows the plots of compressive load versus end shortening. As expected, the shortest length specimen produced the highest buckling load.

The graph indicates that there is little change in the specimen's buckling strength in going from 21 to 24 inches (533 to 610 mm) compared to the change in going from 18 to 21 inches (457 to 533 mm). This exercise gave reasonable assurance that a specimen of length 24 inches (610 mm) can represent the local or shell buckling behavior of a very long tube.

4.3 Buckling Test Results

A typical curve of load versus the end shortening is shown in the third plot of Fig. 4.3. The significance of consecutive ranges along this curve is given below.

1. The arrow in range 1 indicates that the system still has some slack in it, even though the 50 lb. (223N) preload removed most of it.
2. In range 2, the elastic, pre-buckling portion of the curve, the specimen is continuously taking load. It is important to note that the end shortening was measured from an extension of this line down to the 'e' axis.
3. Point 3 indicates the initial buckling load. This is where the specimen first shows visible signs of the developing buckles. The specimens exhibited one of two types of behavior when the initial buckling load was reached. Either they snapped abruptly into the buckled mode, causing a deviation from the straight-line curve, or they very slowly went into

the buckled state, which caused little or no deviation from the straight-line portion. This latter type of behavior is evident, for example in Fig. 4.4.

4. The specimen continues to take more load until it reaches point 4, the peak or collapse load.
5. Point 5 indicates the range in which the specimen is losing load and still collapsing.
6. Point 6 is the point at which the specimen is in the fully buckled state of equilibrium. Further end shortening from this position was not possible.

P versus e curves for selected specimens are shown in Figs. 4.5 through 4.8. Their plots are similar to those in Fig. 4.3 and 4.4. They start with some slack in the system, followed by a linear increase in load until the initial buckling, then take more load until collapse; this being followed by a significant loss in load-carrying capability.

Each of Figs. 4.5 through 4.8 contains six plots, two for each of three loading rates. The rates are indicated at the top of these pages. Also, on each curve, the initial buckling load, as observed, is indicated by an arrow. The end shortening for each individual test is of course found on the absissa as the difference between final and initial values of e.

The equipment appeared to operate stably if it was allowed about one hour to warm up. As mentioned previously, a backlash was developed in the system due to the addition of the amplifier, inductors, and capacitors which boosted the input and filtered out much of the noise. Even though the specimens were preloaded to 50 pounds (223 N) to compensate for the backlash, some backlash can still be seen in the plots of the P versus e curves.

to increase its buckling load. The mediocre quality of the laboratory specimens used in this program, on the other hand, made them susceptible to significant effects of out-of-roundness and other imperfections to which cylincer buckling is known to be sensitive and would reduce the buckling loads. Also the presence of slots probably tended to reduce the buckling loads, as well.

The best that can be said in characterizing the values obtained, in aggregate, is that virtually all lie between 0.5 and 1.5 times the theoretical value for circular cylinders of the same curvature. This would make them stiffer, by perhaps two to three times the circular cylinders with which they are being compared.

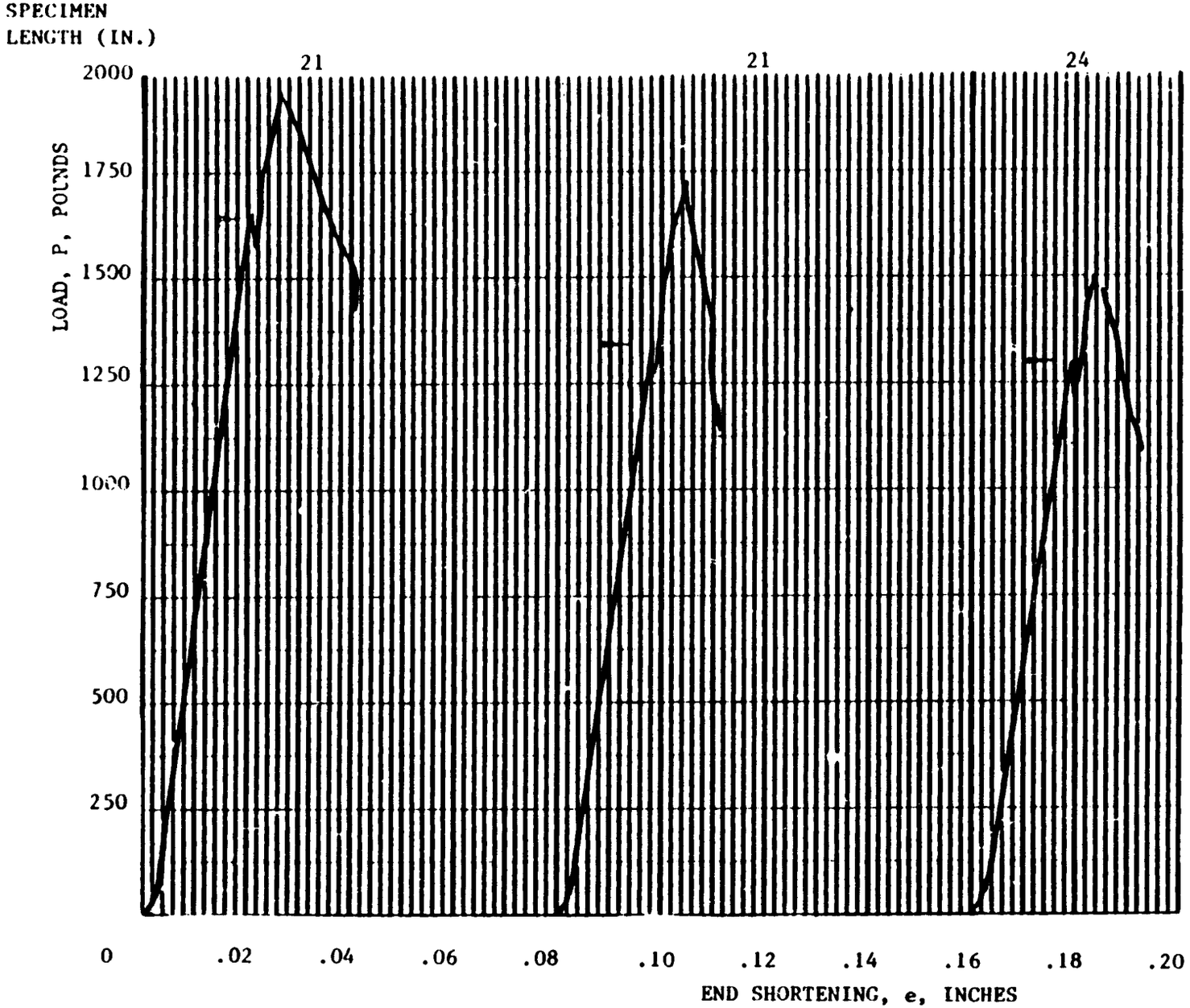

FIG. 4.1 COMPRESSIVE LOAD VERSUS END SHORTENING; SPECIMEN NE-1 FOR DETERMINATION OF REQUIRED SPECIMEN LENGTH

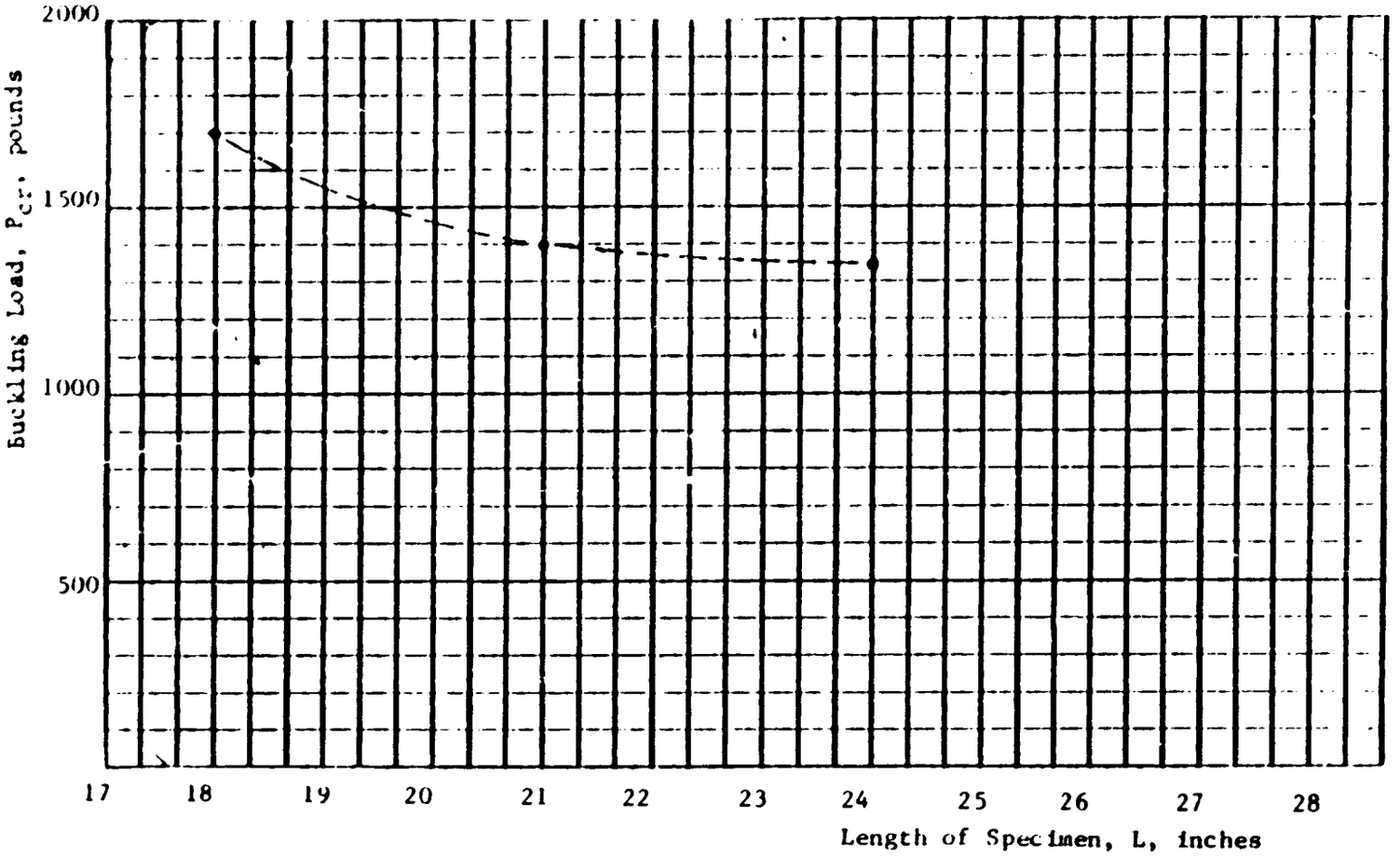

Fig. 4.2 Buckling Load versus Specimen Length

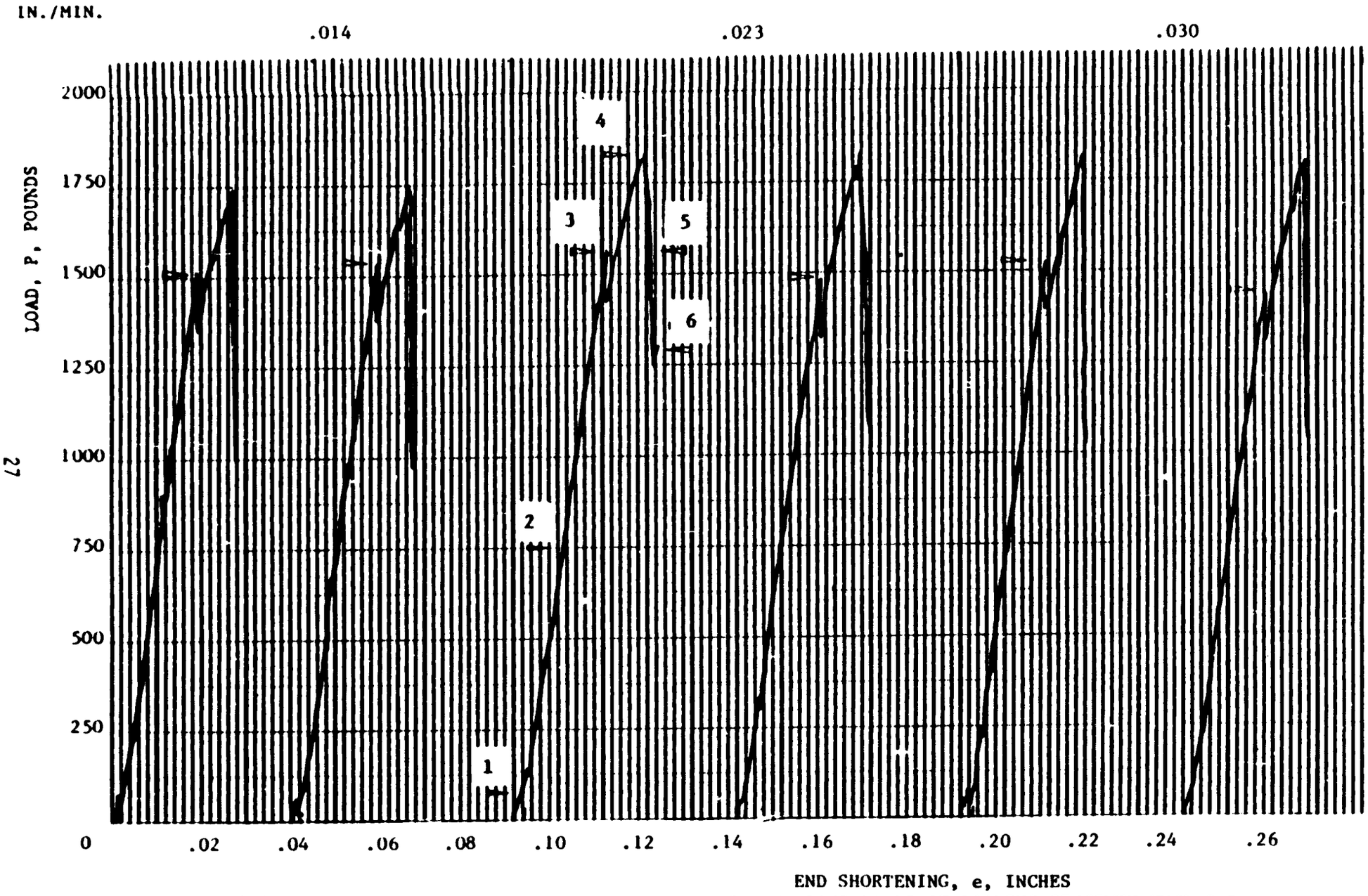

FIG. 4.3 COMPRESSIVE LOAD VERSUS END SHORTENING FOR VARIOUS RATES OF LOADING SPECIMEN UNCL-2-B

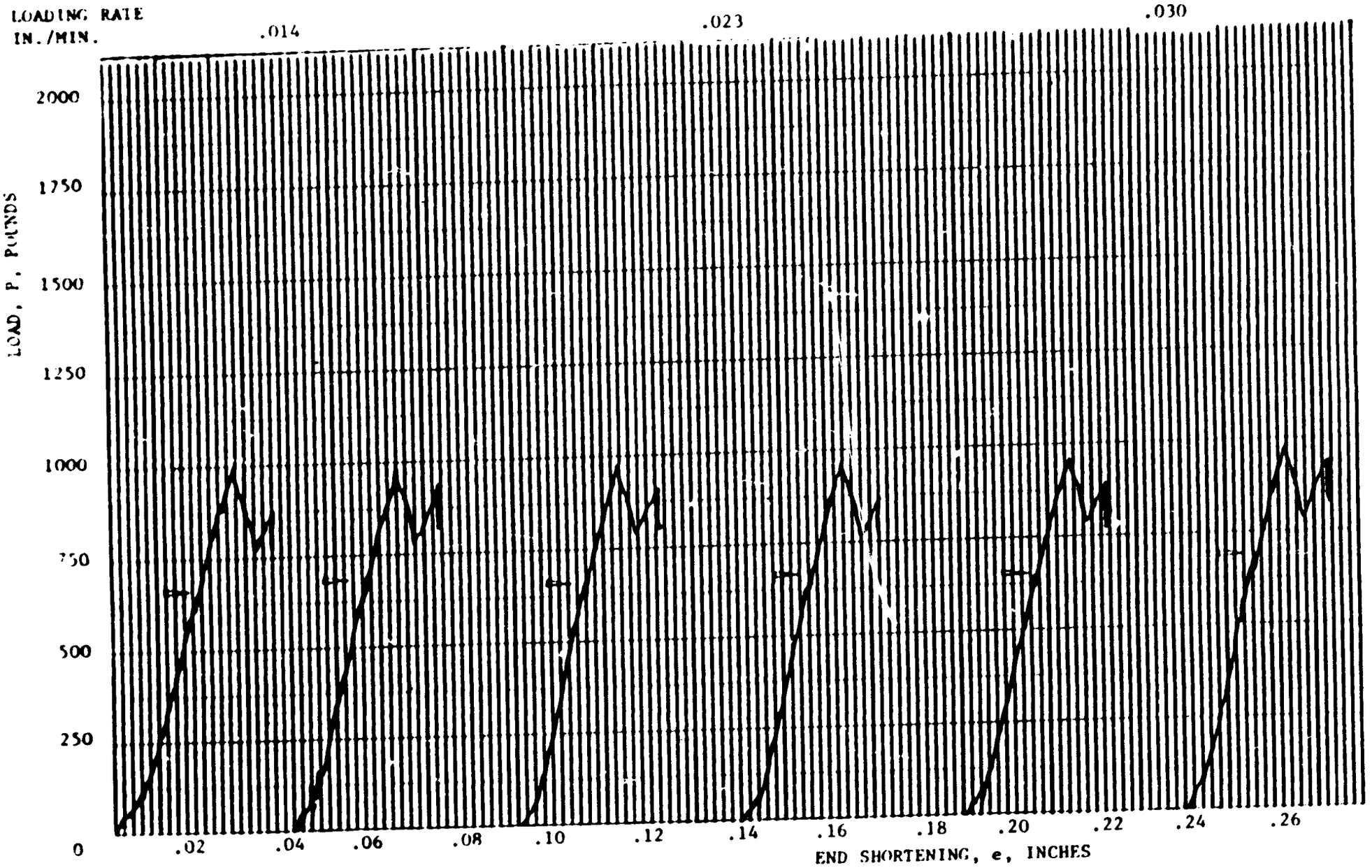

FIG. 4.4 COMPRESSIVE LOAD VERSUS END SHORTENING FOR VARIOUS RATES OF LOADING SPECIMENT ND-1; SMALL RADIUS AND MODERATELY FLAT (R=1.65", f=0.50)

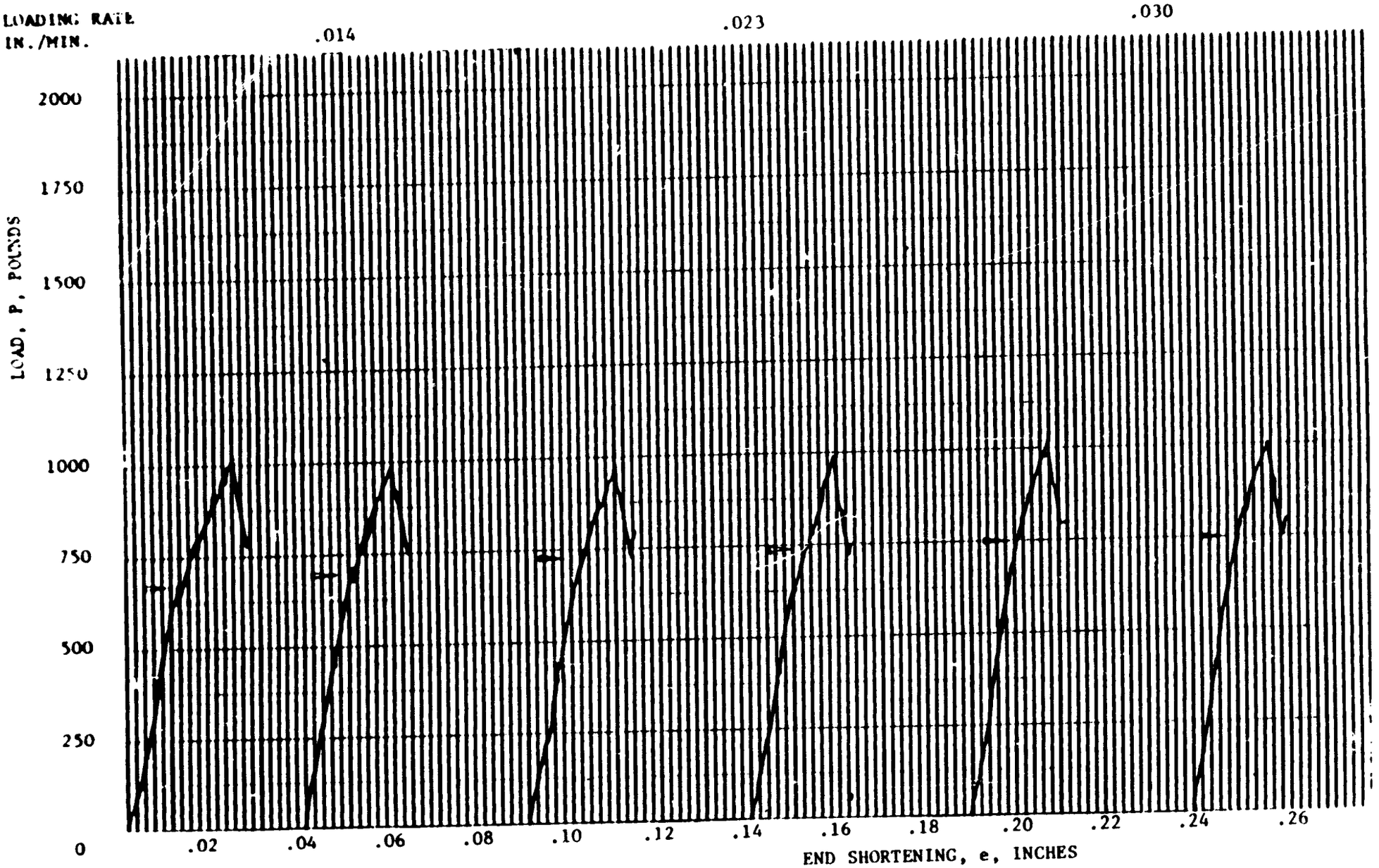

FIG. 4.5 COMPRESSIVE LOAD VERSUS END SHORTENING FOR VARIOUS RATES OF LOADING SPECIMEN NB-5; LARGE RADIUS AND VERY FLAT (R=3.56, f=0.63)

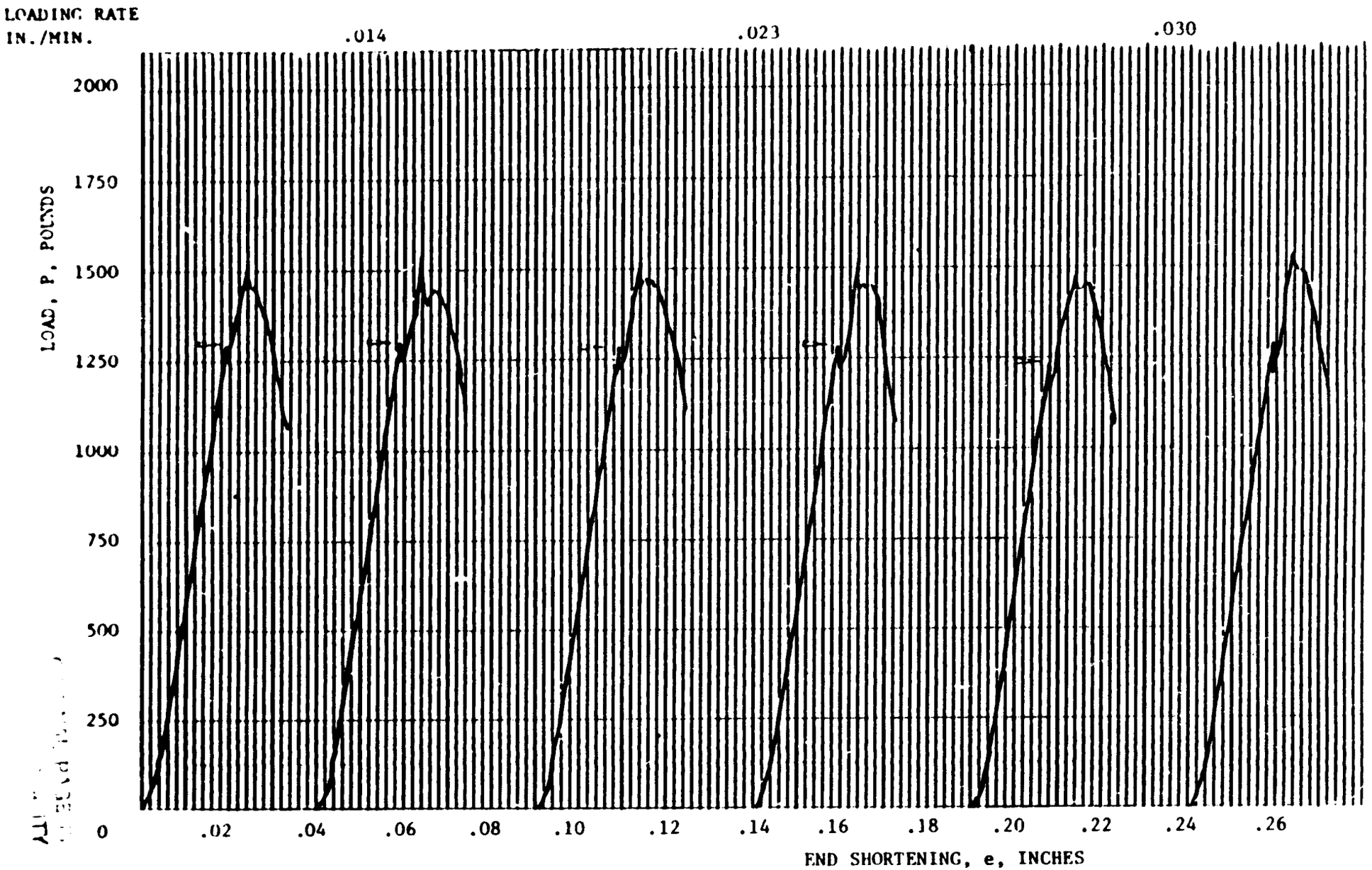

FIG. 4.6 COMPRESSIVE LOAD VERSUS END SHORTENING FOR VARIOUS RATES OF LOADING SPECIMEN NE-1; LARGE RADIUS AND MODERATELY FLAT (R=2.76", f=0.51)

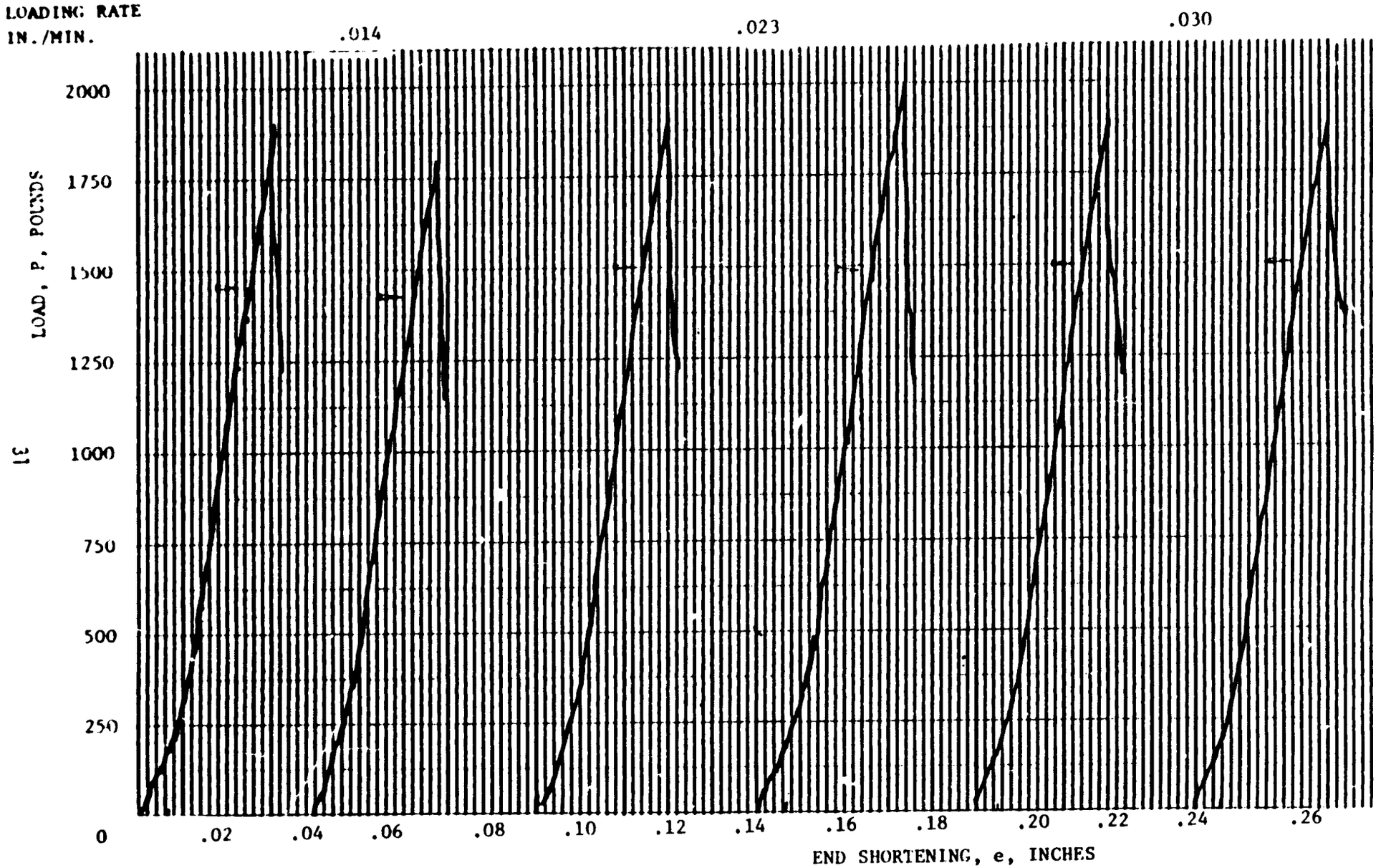

FIG. 4.7 COMPRESSIVE LOAD VERSUS END SHORTENING FOR VARIOUS RATES OF LOADING SPECIMEN NG-2; SMALL RADIUS AND SLIGHTLY FLAT (R=2.00", f=0.28)

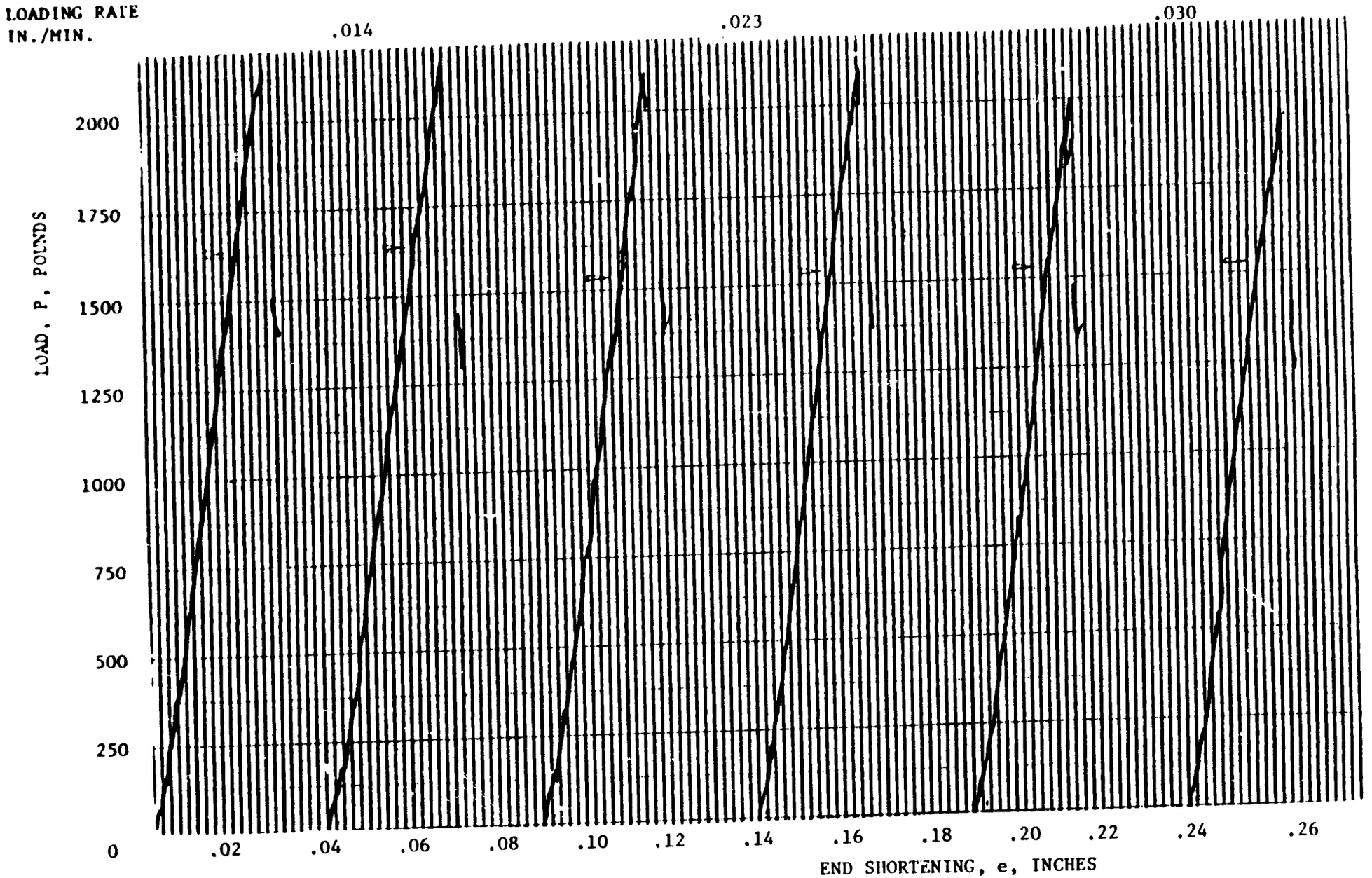

FIG. 4.8 COMPRESSIVE LOAD VERSUS END SHORTENING FOR VARIOUS RATES OF LOADING SPECIMEN NH-1; SMALL RADIUS AND ALMOST ROUND (R=2.00, f=0.17)

TABLE 4.2

BUCKLING STRESS· SPECIMEN/CYLINDER

SPECIMEN	Buckling Stress of Circular Cylinder 0.6Et/R, psi	Initial Buckling Stress	$\frac{\sigma \text{ cr, bfet}}{\sigma \text{ cr, cyl}}$
NF-4	11083	6628	.598
ND-1	10546	5988	.567
NH-4	9355	5478	.585
NC-3	9255	7975	.862
NH-1	8700	9572	1.1
NH-2	8700	8429	.968
E-6-A	8700	10107	1.162
E-6-B	8700	7643	.878
NG-2	8700	9597	1.103
NG-4	8131	7500	.922
UNCL-2	7632	8834	1.157
UNCL-3	7632	10500	1.357
NG-3	7250	8309	1.146
NG-5	7190	3356	.466
UNCL-1	7016	6003	.855
NE-2	6421	7493	1.167
NE-1	6305	8440	1.338
NB-4	4929	7425	1.506
NB-5	4888	4286	.876
NB-3	4628	5260	1.136

Fig. 4.9 Specimen Buckling During Test

After preloading and adjusting, each specimen was loaded and observed with the initial buckling load determined visually. Fig. 4.9 is a photograph of a specimen during buckling. Close observation will reveal the presence of diamond shape buckles taking form. The three different rates of loading were applied to determine if rate-of-loading had any effect on the buckling strength or behavior of the specimen. As can be seen in the plots of Figs. 4.4 through 4.8, there was little overall difference between the results for the three rates of loading. Therefore, the lowest rate, 0.014 in/min (.356 mm/min) was used in reducing the data. The collapse loads ranged from 900 to 2,000 lb (4,000 to 8900 N) and the initial buckling loads from 700 to 1,800 pounds (3115 to 8010 N). Table 4.1 provides a summary of the buckling test results. The specimens are listed in ascending order according to their radii of curvature. For standardization with other buckling data and comparison with theory, the plot of the buckling stress versus the radius of curvature is presented in dimensionless form, see Fig. 4.10, with the initial buckling stress of the BFET divided by the buckling stress of a circular cylinder (same radius) plotted against radius of curvature divided by the specimen thickness. The numerical data for Fig. 4.10 is given in Table 4.2. It is perhaps an expected result that while the buckling stress for circular cylinders is inversely proportional to the radius of curvature, this is not the case with the BFET. The inverse proportionality of buckling load to the radius also applies to non-circular cylinders, where the inverse of the maximum radius of curvature is an accepted proportionality factor. However, the BFET is a more complex shape, and while its cross-section does contain only one radius of curvature (that of each of the six adjoining arcs), it has clamped edges which would be expected

TABLE 4.1

SUMMARY OF BUCKLING TESTS

SPECIMEN	@ Collapse (in.) END SHORTENING	(Pounds) BUCKLING LOAD	COLLAPSE (Pounds) LOAD
NF-4	.018	769	1063
ND-1	.022	713	1032
NH-4	.0205	932	1275
NC-3	.0215	925	1363
NH-1	.025	1675	2207
NH-2	.022	1475	1878
NE-6	.0265	1769	1888
NE-7	.02	1338	1644
NG-2	.0235	1488	1900
NG-4	.0215	1313	1750
UNCL-2	.012	1325	1450
UNCL-3	.0245	1575	1800
NG-3	.0205	1413	1638
NG-5	.0285	682	1788
UNCL-1	.012	913	1138
NE-2	.022	1282	1438
ME-1	.022	1350	1584
NB-4	.026	1225	1719
NB-5	.0205	750	1050
NB-3	.01	863	988

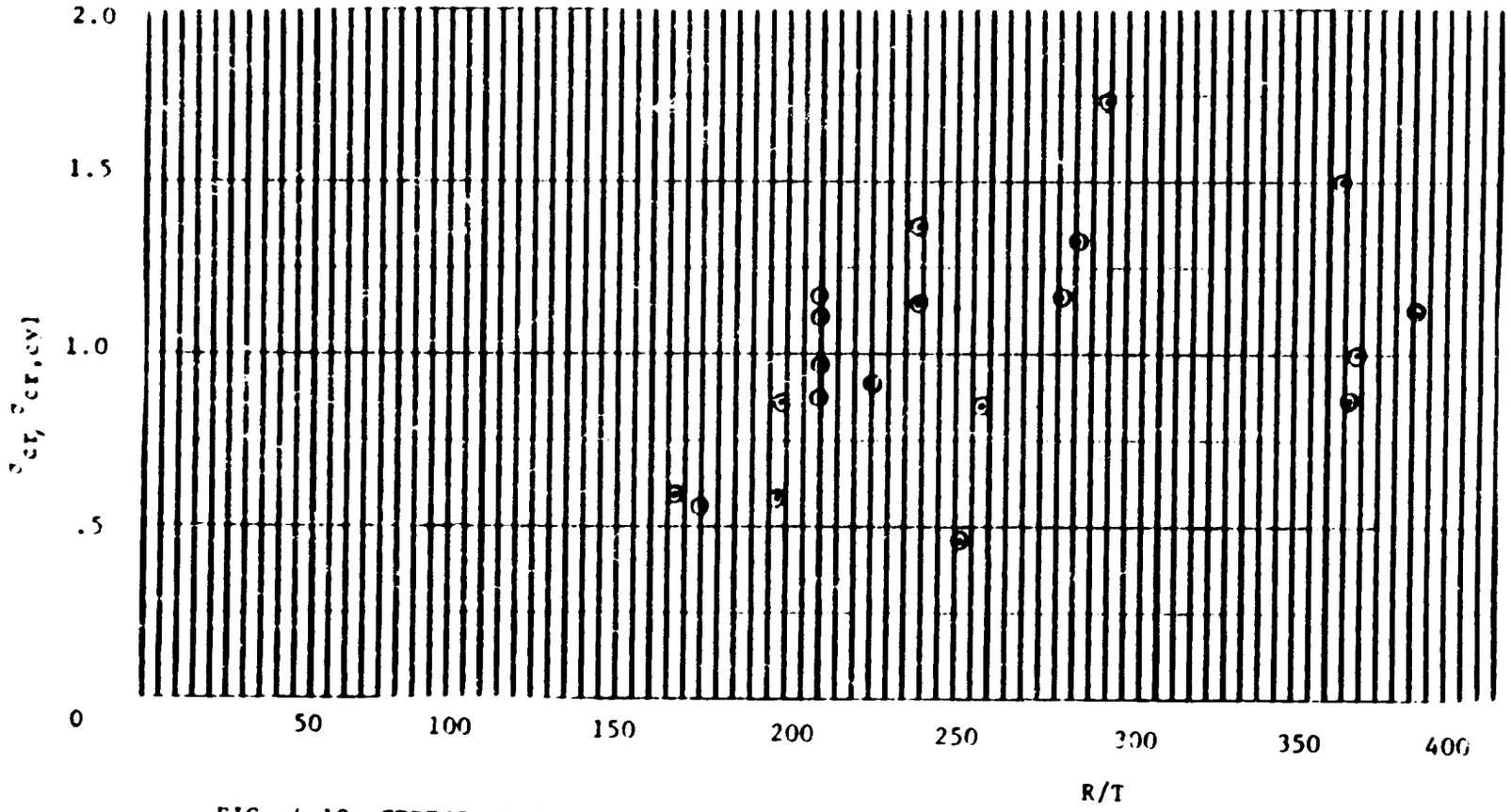

FIG. 4.10 STRESS AT INITIAL BUCKLING/ BUCKLING STRESS OF CIRCULAR CYLINDER VERSUS RADIUS OF CURVATURE/ THICKNESS

5. CONCLUSION

It has been demonstrated in this phase of the investigation that the bi-convex foldable elastic tube is a viable type of structural member, even though the slots needed for successful deployment lower the flexural, torsional and buckling strengths slightly. While the initial buckling strengths in this program ranged from 700 to 1800 lbs (3.11 to 8.01 KN), it is felt that greater loads could have been realized with more refined equipment and fabrication processes. The authors recommend that more test specimens with more widely varying cross-sections be tested. Ideally, the slots and end plates should be fabricated in a machine shop. A few of these specimens should be earmarked for strain measurement also. Finally, a rigorous theoretical and experimental analysis, run on the specimens to determine the stress concentrations around the slots would be beneficial to the establishment of design criteria.

REFERENCES

1. Gertsma, L.W., Dunn, J.H., Kempke, E.E., Jr.: Evaluation of One Type of Foldable Tube, NASA TM X-1187, December 1965.

2. Crawford, R.F.: Strength and Efficiency of Deployable Booms for Space Applications, AIAA Paper No. 71-396, Variable Geometry and Expandable Structures Conference, April 1971.

3. Fernandez-Sintes, J., Cristos, J.C.: Foldable Elastic Tubes for Hinges on Satellites, Contractor Report ESRO-CR 65 by Instituto Nacional de Tecnica Aerospacial, Madrid, Spain, for the European Space Research Organization, February 1973.

4. Jones, I.W., Boateng, C., Williams, C.D.: Foldable Elastic Tubes for Large Space Structure Applications, Final Report-Phase I, Grant NSG 1320, NASA Langley Research Center, January 1980.

5. Boateng, C.: Deployment Tests for One Type of Foldable Elastic Tube (BFET), Master's Degree Thesis, Howard University, December 1979.

6. Jones, I.W., Williams, C.D.: Foldable Elastic Tubes for Large Space Structure Applications, Final Report-Phase II, Grant NSG 1320, NASA Langley Research Center, January 1981.

7. Williams, C.: Experimental Evaluation of Foldable Elastic Tubes Modified with Stress Alleviating Devices, Master's Degree Thesis, Howard University, February 1981.

8. Mikulus, M.M., Bush, H.G., Card, M.F.: Structural Stiffness, Strength and Dynamic Characteristics of Large Tetrahedral Space Truss Structures, NASA TM X-74001, March 1977.